ARTICLES
https://doi.org/10.1038/s41560-022-01019-4
nature energy

Check for updates

OPEN

Reversible hydrogenation of carbon dioxide to formic acid using a Mn-pincer complex in the presence of lysine

Duo Wei[1], Rui Sang[1], Peter Sponholz[2]✉, Henrik Junge[1]✉ and Matthias Beller[1]✉

Efficient hydrogen storage and release are essential for effective use of hydrogen as an energy carrier. In principle, formic acid could be used as a convenient hydrogen storage medium via reversible CO_2 hydrogenation. However, noble metal-based catalysts are currently needed to facilitate the (de)hydrogenation, and the CO_2 produced during hydrogen release is generally released, resulting in undesirable emissions. Here we report an α-amino acid-promoted system for reversible CO_2 hydrogenation to formic acid using a Mn-pincer complex as a homogeneous catalyst. We observe good stability and reusability of the catalyst and lysine as the amino acid at high productivities (CO_2 hydrogenation: total turnover number of 2,000,000; formic acid dehydrogenation: total turnover number of 600,000). Employing potassium lysinate, we achieve >80% H_2 evolution efficiency and >99.9% CO_2 retention in ten charge–discharge cycles, avoiding CO_2 re-loading steps between each cycle. This process was scaled up by a factor of 18 without obvious drop of the productivity.

As the most significant greenhouse gas, carbon dioxide (CO_2) has risen from pre-industrial levels of 280 ppm (parts per million) to 419 ppm in the Earth's atmosphere in February 2022, along with the exponential global energy demand supplied by carbon-rich fossil fuels (Supplementary Fig. 1)[1,2]. The extensive CO_2 valorization and zero-CO_2 emission technologies are crucial to mitigate global warming and related climatic deterioration. To accomplish such purpose, 196 countries/parties have signed the 2015 Paris Agreement committing to reach net-zero CO_2 emissions around the year 2050. Generally, there are two approaches to realize carbon neutrality: reducing carbon emissions by shifting towards alternative energy technologies and balancing carbon emissions with carbon usage.

In this context, the feasibility study of hydrogen (H_2) as a clean alternative energy carrier has inspired growing attention because it could be prepared from renewable resources, for example, by electrochemical water splitting, and produces nothing but water and energy in fuel cells[3,4]. However, it is troublesome to transport and store hydrogen gas due to its physical and explosive properties in mixtures containing oxygen. This situation can be solved by converting hydrogen gas to solid or liquid organic hydrogen carriers[5,6], for example, by catalytic CO_2 hydrogenation. Following this concept, besides methanol and Fischer–Tropsch products (hydrocarbons), formic acid (HCO_2H, FA) and its formate salts also are readily accessible. Both are stable compounds that can be stored and dehydrogenated on demand to H_2 and CO_2 under milder conditions compared with other liquid organic hydrogen carriers (Fig. 1a)[7–9], separating hydrogen storage and release without the restriction of time and place. It should be noted that hydrogen is wasted partly in the form of water when it is stored in methanol, which is not the case for formic acid, even though the hydrogen content in FA (4.4 wt%) is lower than that in methanol (12.6 wt%). Overall, a FA-based H_2 storage and release system may also benefit from the CO content in the generated hydrogen (usually less than 10 ppm), which is important for its application in fuel cells.

An electric battery is commonly a source of electric power containing electrochemical cells to power electronic products. Therefore, reusable electric batteries can be discharged and recharged multiple times under electric current. According to this concept, a chemical hydrogen battery is a device where energy is stored in the form of hydrogen that is discharged and recharged as needed. Hydrogen is directly converted to electric energy by using fuel cell technologies after its release out of the chemical hydrogen battery. Obviously, such technology offers substantial potential as a clean energy technology working towards carbon neutrality.

Only limited examples of such chemical hydrogen batteries have been demonstrated to date. Clearly, catalysts active in both hydrogenation and dehydrogenation reactions are essential and only a few molecularly defined transition metal-based complexes are known to fulfil this mission. Most systems contain expensive noble metal-based catalysts, for example, Rh (ref. [10]), Ru (refs. [11–18]) and Ir (refs. [19,20]) (Supplementary Fig. 2). An example of a heterogeneous catalyst was reported in 2016 when a reusable bimetallic catalyst was developed to hydrogenate and dehydrogenate *N*-heterocycles efficiently[21]. Besides, it's difficult to reach a simple and truly rechargeable hydrogen storage and release device when it comes to non-unified reaction conditions in H_2 recharge and discharge steps, for example, catalysts, solvents[11,22], bases change[20], pH control[19], reloading of storage media (concerning catalysts, H_2 carriers and so on) between each charge–discharge cycle[13] or generally low catalytic efficiency (that is, turnover numbers). Furthermore, in all currently known examples, the release of simultaneously produced CO_2 in the dehydrogenation process results in not only undesirable carbon emissions but also inferior H_2 purity for subsequent fuel cell applications[13,15]. Consequently, there is an actual demand for carbon-neutral hydrogen storage and release technologies that integrate the carbon capture (recycling the released CO_2, dotted arrows in Fig. 1b) or in an ideal condition avoid CO_2 release in the dehydrogenation reactions (bold arrows in Fig. 1b).

[1]Leibniz-Institut für Katalyse e.V., Rostock, Germany. [2]APEX Energy Teterow GmbH, Rostock-Laage, Germany. ✉e-mail: Peter.Sponholz@apex-energy.de; henrik.junge@catalysis.de; matthias.beller@catalysis.de

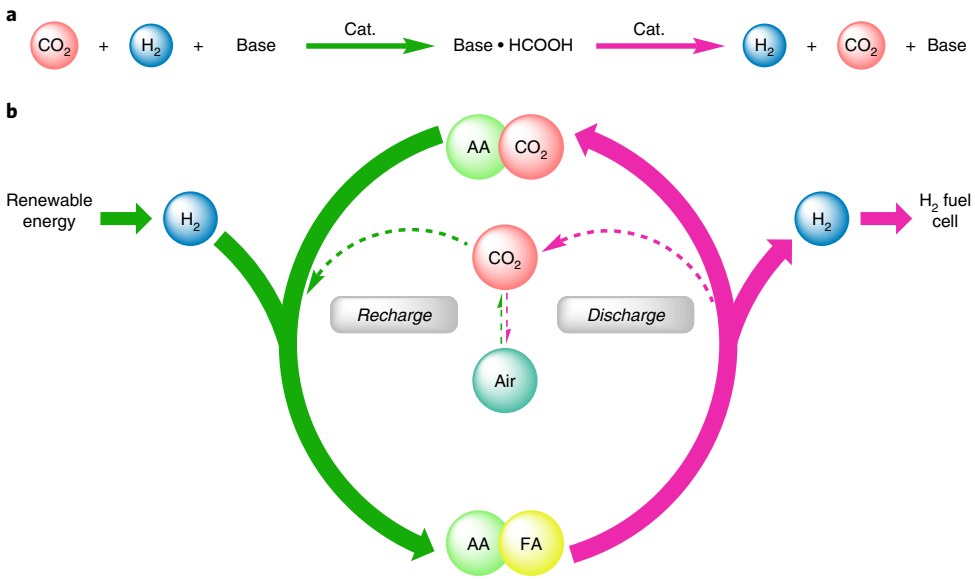

Fig. 1 | Illustration of hydrogen storage and release based on formic acid. a, Catalytic CO_2 hydrogenation to formic acid and its dehydrogenation to H_2 and CO_2 in the presence of bases. Cat., Catalyst. **b**, Concept of the carbon-neutral chemical hydrogen storage and release described in this work. The chemical hydrogen storage and release is based on the interconversion of CO_2, amino acid (AA), H_2 and FA. Retaining CO_2 in the cycle (bold arrows) is advantageous compared with CO_2 recycling (dotted arrows). Green arrows represent recharge, while pink ones show discharge.

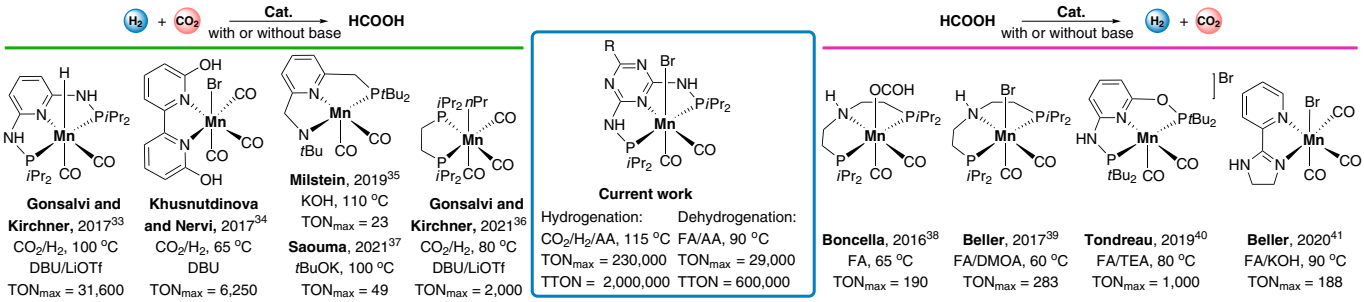

Fig. 2 | Homogeneous Mn complexes applied in CO_2 hydrogenation to FA[33–37] and its dehydrogenation reactions[38–41]. Hydrogenation reactions are shown on the left side of the figure under the green bar, and dehydrogenation is shown on the right under the pink bar. DBU: 1,8-diazabicyclo(5.4.0)undec-7-ene, DMOA: *N,N*-dimethyloctylamine, TEA: triethylamine, AA: α-amino acid, FA: formic acid, TON_{max}: turnover number, TTON: total turnover number.

The homogeneous catalyst development for the two individual steps of chemical hydrogen storage and release—CO_2 hydrogenation to FA[23] and its dehydrogenation processes[7]—focused traditionally on noble metals. However, non-noble metal-based complexes have been proven to be valuable, more recently[24,25]. In this context, apart from iron[9,26], manganese especially is of important interest, owing to its abundant, non-toxic, biocompatible and environmentally friendly features[27]. However, Mn pincer complexes were first recognized for catalytic hydrogenation reactions in 2016[28–32]. Thus, examples of homogeneous Mn catalysts for CO_2 hydrogenation to FA[33–37] and its dehydrogenation[38–41] are rather limited and often come with far lower catalytic efficiency compared with their noble-metal counterparts (Fig. 2). Most important of all, Mn catalysts are rarely reported so far to be efficient in both CO_2 hydrogenation to FA and its dehydrogenation under unified reaction conditions (same catalyst, base, solvent and so on). Recently, a ruthenium-catalysed CO_2 fixation to formates in the presence of amino acids (AAs) was reported by our group[42]. We speculated that such a system could also be used to develop state-of-the-art carbon-neutral hydrogen storage and release instead of using conventional CO_2 absorbents, for example, alkanolamines[43]. Among the tested AAs, lysine (Lys) offers several advantages for the fixation of CO_2 as it is an essential AA, industrially produced from microbial fermentation with >2.2 million tonnes scale per year[44].

Herein we provide a sustainable hydrogen storage and release method integrating the reversible hydrogenation of CO_2 to FA and carbon capture processes. In our catalytic system, we use the α-amino acid Lys and a specific manganese complex as the carbon absorbent and catalyst. We show that such a system can catalyse the reversible hydrogenation of CO_2 to FA in high productivities. With potassium lysinate, we achieve high evolution efficiency of hydrogen and retain CO_2 inside of the cycles.

Catalytic CO_2 hydrogenation

Initially, using several manganese, iron, cobalt, and rhenium complexes with bidentate and tridentate ligands, we performed the Lys-promoted CO_2 hydrogenation (Supplementary Table 1). Under standard reaction conditions, CO_2 (20 bar) hydrogenation happened in the presence of Lys (5.0 mmol) in H_2O:THF (5:5 ml, THF: tetrahydrofuran) with 60 bar H_2 at 145 °C and 12 h (Table 1 and Supplementary Figs. 3–5 and 50). Among all the tested catalysts, Mn–PNP–Br complexes 1–3, and 5–7 proved to be the most

Table 1 | Mn-catalysed CO_2-to-formate transformation

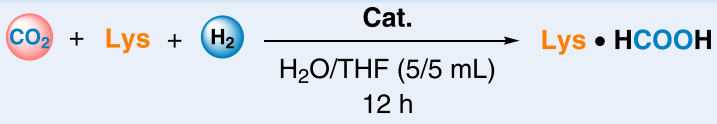

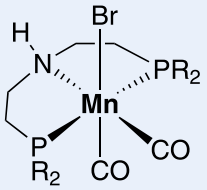

R = *i*Pr, **Mn-1**
R = Cy, **Mn-2**
R = Ph, **Mn-3**
R = *t*Bu, **Mn-4**

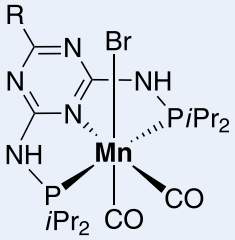

R = Me, **Mn-5**
R = NH-C_3H_5, **Mn-6**
R = $(CH_2)_2$-1-imidazolyl, **Mn-7**

Entry	Cat. (μmol, ppm)	Formate (mmol)	% yield	TON
1	Mn-1 (0.10, 20)	4.0	80	40,000
2	Mn-2 (0.10, 20)	3.8	76	38,000
3	Mn-3 (0.10, 20)	2.5	50	25,000
4	Mn-4 (0.10, 20)	0.03	<1	300
5	Mn-5 (0.10, 20)	4.3	86	43,000
6	Mn-6 (0.10, 20)	4.4	88	44,000
7	Mn-7 (0.10, 20)	4.3	86	43,000
8	Mn-5 (0.02, 4)	0.3	6	15,000
9	Mn-6 (0.02, 4)	3.0	60	150,000
10	Mn-7 (0.02, 4)	0.9	18	45,000
11[a]	Mn-6 (0.02, 4)	4.6	92	230,000
12[b]	Mn-6 (0.02, 4)	4.0	80	200,000
13[b,c]	Mn-6 (0.02, 4)	1.3	26	65,000

General conditions: Lys (5.0 mmol), Mn catalyst (0.02 or 0.10 μmol; Cat.), H_2O:THF (5:5 ml), CO_2:H_2 (20:60 bar), 145 °C, 12 h. [a] 115 °C. [b] 85 °C. [c] H_2 (40 bar). Amount of formate product is determined by ^{1}H NMR with DMF (250 μL, 3.24 mmol) as internal standard (NMR, nuclear magnetic resonance spectroscopy; DMF, dimethylformamide). Yield of formate is calculated by (mmol formate)/(mmol Lys)×100%. TON of formate is calculated by (mmol formate)/(mmol catalyst). The gas mixtures were analysed by gas chromatography (GC), and no concomitant CO/CH_4 was found. All experiments were performed at least twice (Supplementary Table 1); average values are shown (standard deviation ≤10%, except for entry 8, which is 28%).

efficient ones (PNP: PNP pincer ligand). Remarkably, using Mn-1, 2 and 3 (refs. [28,45,46]) (0.10 μmol, 20 ppm, based on Lys), up to 4.0 mmol Lys ammonium formate were produced (80% yield based on Lys; turnover number (TON) 40,000, Table 1, entries 1–3). On the other hand, Mn-4, bearing *t*-butyl substituents at the phosphorus atoms, resulted in no detectable formate. To our delight, Mn–PN^{5}P^{iPr}–Br complexes Mn-5, 6 and 7 (ref. [29]) led to improved formate yields up to 88% and TONs up to 44,000 (Table 1, entries 5–7). Decreasing the catalyst loading to only 0.02 μmol (4 ppm), Mn-6 gave formate in slightly lower yield of 60%, but a TON of 150,000 was achieved (Table 1, entry 9). Applying the same quantity of Mn-5 and Mn-7, however, resulted in much lower yields (Table 1, entries 8 and 10). Therefore, we focused on Mn-6 in subsequent experiments. Fortunately, formate was produced even at 85 °C and 115 °C, leading to high yields (80% and 92%, respectively) and TONs (200,000 and 230,000, respectively, Table 1, entries 11 and 12). However, reducing the initial hydrogen pressure from 60 bar to 40 bar drastically decreased both yield and TON (Table 1, entry 13). Utilizing [$Mn(CO)_5Br$] or other Mn pincer and bidentate complexes and the respective iron, cobalt and rhenium analogues as catalysts, formate was detected in <1% yield (Supplementary Table 1, entries 8–18).

CO_2 hydrogenation in the presence of 16 other AAs and organic and inorganic bases led to much lower formate yields, revealing the specific role of Lys in CO_2 hydrogenation reactions (Supplementary Tables 2–3). Only when using another basic AA arginine (Arg) bearing a guanidino group in its side chain, formate is produced in 62% yield.

Catalytic dehydrogenation of formic acid

Next, we investigated the H_2 evolution from formic acid (5.0 mmol) in the presence of Lys (1.0 equivalent) at 90 °C using the Mn catalysts previously active in the hydrogenation step. The Mn-PN$^{(H)}$P–Br complexes Mn-1, 2 and 3 promoted the H_2 formation in yields up to 70% equivalent to 3.5 mmol H_2 and TON 17,500 (Table 2, entries 1–3). Again, Mn–PN^{5}P^{iPr}–Br (Mn-6) catalysed the H_2 release more efficiently with quantitative H_2 yield and a TON of 29,400, while Mn-5 and Mn-7 gave obviously lower productivities (Table 2, entries 4–6). Lowering the quantity of Mn-6 to 0.10 μmol (20 ppm), the conversion was incomplete with much lower productivity (Table 2, entry 7). Decreasing the temperature to 85 °C, 74% yield and TON >21,000 were still obtained (Table 2, entry 8). Compared with Lys, Arg was found to be less active, leading to H_2 in 46% yield (Table 2, entry 9). Utilizing the potassium salt of Lys (LysK), a high yield of H_2 also was achieved (94%, Table 2, entry 10). In addition, Table 2 shows the H_2:CO_2 molar ratios in the gas products that contain generally less than 50% CO_2, demonstrating again the good

Table 2 | Mn-catalysed FA dehydrogenation

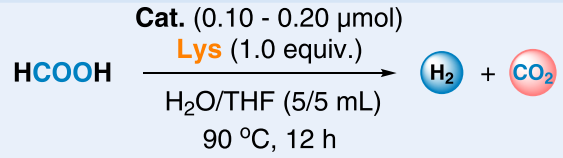

Entry	Cat. (μmol, ppm)	V_{gas} (ml)	H_2:CO_2 (%)	H_2 (mmol)	% yield	TON
1	Mn-1 (0.20, 40)	116	74:26	3.5	70	17,500
2	Mn-2 (0.15, 31)	52	81:19	1.7	34	11,300
3	Mn-3 (0.16, 32)	28	64:36	0.7	14	4,300
4	Mn-5 (0.18, 37)	38	74:26	1.1	22	6,100
5	Mn-6 (0.17, 34)	158	78:22	5.0	99	29,400
6	Mn-7 (0.16, 32)	22	55:45	0.5	10	3,100
7	Mn-6 (0.10, 20)	18	70:30	1.0	20	10,000
8[a]	Mn-6 (0.17, 34)	125	73:27	3.7	74	21,700
9[b]	Mn-6 (0.17, 34)	72	76:24	2.3	46	13,500
10[c]	Mn-6 (0.17, 34)	115	>99.9:0.1	4.7	94	27,600

General conditions: FA (5.0 mmol), Lys (5.0 mmol), Mn catalyst (0.10–0.20 μmol), H_2O:THF (5:5 ml), 90 °C, 12 h, 100 ml autoclave. [a] 85 °C. [b] Arg instead of Lys. [c] LysK instead of Lys. Volume and content of the gas phase are analysed by manual burettes and GC, respectively, after correction by the blank volume. CO is not detectable in all cases (below the CO quantification limit of 10 ppm). Yield of H_2 is calculated by (mmol H_2)/(mmol HCOOH)×100%. TON of H_2 is calculated by (mmol H_2)/(mmol catalyst). V_{gas}, volume of generated gases. All experiments were performed at least twice (Supplementary Table 17); average values are shown (standard deviation <10%, except for entry 6, which is 12%).

CO_2 capture effect induced by Lys in the FA dehydrogenation reactions. Notably, LysK led to >99.9% CO_2 retention, which offers the possibility for further reuse of CO_2.

Additionally, blank reactions reveal that in the absence of Mn-6 or Lys, no product was detected (Supplementary Tables 4 and 9). Applying FA/LysK mixtures in the presence of other organic solvents, for example, 2-methyl-THF, triglyme and ethanol, H_2 was produced in up to 88% yield with >99% CO_2 retention (Supplementary Table 14 and Supplementary Fig. 38). In addition, H_2 evolution from FA/LysK mixtures in an open system (using a manual burette) presented a complete FA conversion within 3 h, which resulted in a higher CO_2 ratio (14%, Supplementary Figs. 39–41). Time-dependent experiments of CO_2 hydrogenation and FA dehydrogenation applying Lys and Mn-6 were performed (Supplementary Table 16). Slightly decreased formate yield in the CO_2 hydrogenation reaction was observed at 90% in 6 h, which dropped to 12% in 3 h. On the other hand, performing the FA dehydrogenation reaction in a shorter time led to decreased H_2 yields (72% in 6 h and 4% in 3 h).

Reusability of Mn catalyst

To avoid extra addition of catalysts or bases between the H_2 storage–release cycles, we investigated the reusability of catalyst and base beforehand (Fig. 3). Based on the biphasic solvent system (Supplementary Fig. 26), we achieved a facile recycling of the Mn catalyst and organic solvent by separation of the organic and aqueous layers. Therefore, catalyst Mn-6 could be reused for ten consecutive runs in hydrogenation of CO_2 to formate reactions. About 80% of the initial productivity remains after ten runs, resulting in a remarkable total TON (TTON) of 2,050,000 for formate production (Fig. 3a and Supplementary Table 8). The decrease of formate yield is probably due to the incomplete catalyst separation between each run rather than catalyst deactivation as no free phosphine ligand is detected by ^{31}P NMR in the separated organic phase.

Then, we evaluated the reusability of Mn-6 as well as Lys in FA dehydrogenation (Fig. 3b). After each run, a new batch of FA was reloaded into the reaction mixture (first to fifth runs: 5.0 mmol FA and sixth to tenth runs: 20.0 mmol FA). Following this procedure, Mn-6 catalyst and Lys were reused for ten consecutive runs. Fortunately, more than 89% of the theoretical H_2 productivity was achieved, resulting in an excellent TTON of 676,700 for hydrogen. Moreover, the H_2:CO_2 molar ratios in the gas phase are found to be approaching the theoretical value 50:50 after ten runs (Supplementary Table 10 and Supplementary Figs. 29–31). Besides recycling the Mn-6/Lys catalyst system in up to ten runs, the stability in long-term storage was evaluated. Quantitative H_2 yield in FA dehydrogenation was obtained after storing the corresponding reaction solution for two weeks at room temperature under argon. Overall, these results demonstrate the high stability and reusability of the Mn-6 catalyst in both the CO_2 hydrogenation and FA dehydrogenation processes.

Hydrogen storage–release cycles applying Lys

Next, we combined CO_2 hydrogenation to formate and its dehydrogenation applied Lys and Mn-6 complex. Due to the CO_2 loss in the H_2 release step, CO_2 was reloaded for each hydrogenation step (Fig. 4a). The H_2 storage–release cycles start from the dehydrogenation of FA: Mn-6 (0.17 μmol), FA:Lys (5.0:5.0 mmol), THF:H_2O (5:5 ml) in a 100 ml autoclave at 90 °C for 12 h. The inside pressure was then carefully released to the manual burettes at room temperature and analysed by GC. Then, CO_2 is reloaded under CO_2 pressure (20 bar for 0.5 h or 2 bar for 6 h). Afterwards, the autoclave was filled with H_2 (80 bar) and heated at 85 °C for 12 h. After the completion of the H_2 storage step, the reactor was subjected to H_2 release. Following this procedure, ten consecutive cycles in total were performed with >90% yield of H_2 evolution (CO_2 reloading at 20 bar). Using lower CO_2 (2 bar) pressure, an average hydrogen yield of >82% is still achieved. Notably, we performed this carbon-neutral hydrogen storage–release methodology even with CO_2 from air (reloading at ambient conditions for 24 h). Following this concept, over 72% yield of H_2 was obtained in ten consecutive cycles (Fig. 4c, Supplementary Table 11 and Supplementary Figs. 32–34). Detailed studies of CO_2 capture with Lys under various conditions show that carbamate species are first produced under air, then are converted further to bicarbonate at higher CO_2 pressure (Supplementary Tables 5–7 and Supplementary Figs. 6–25).

Hydrogen storage–release cycles applying lysinate salts

Even though we performed the hydrogen storage–release cycles with Lys in excellent efficiency, the development of a practical rechargeable chemical hydrogen battery is not yet achieved. Ideally, such devices consist of closed autoclaves containing the hydrogen

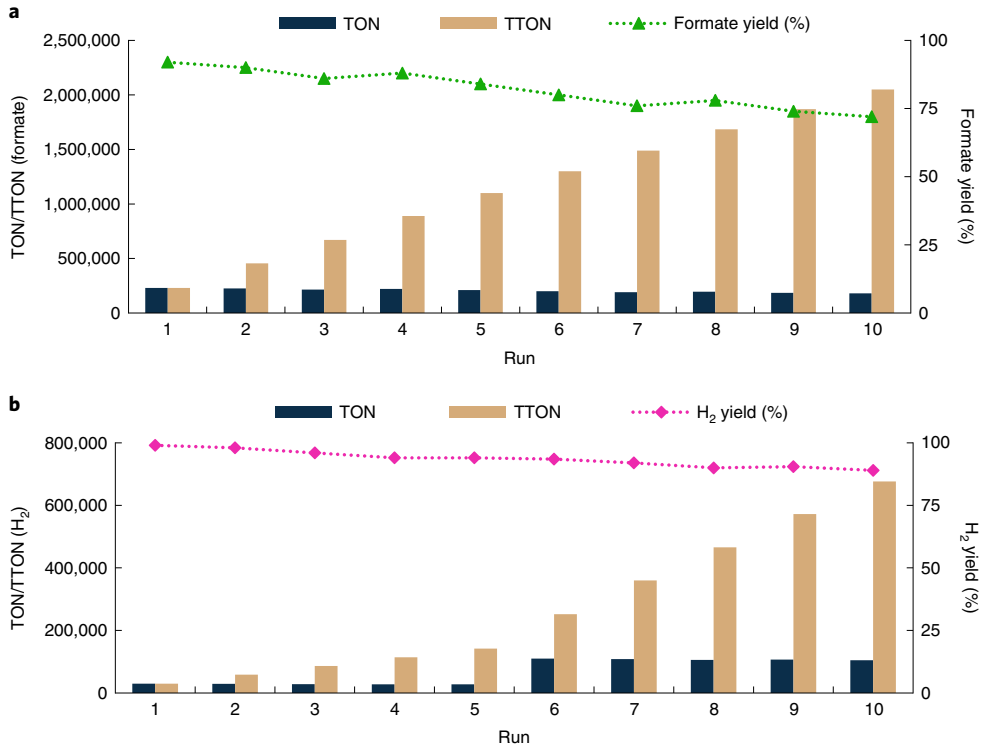

Fig. 3 | Profile of Mn-6 reusability. a,**b**, The reusable performance of Mn-6 catalyst in CO_2 hydrogenation to formate (**a**) and FA dehydrogenation (**b**). Reaction conditions adopted from Table 1, entry 11, and Table 2, entry 5, respectively. The dotted lines serve as guides to the eye.

storage media (in this case, CO_2), where hydrogen is charged and discharged conveniently. Obviously, the reloading of the storage media in this system between each cycle should be avoided as far as possible because it requires additional feedstock, energy input and reaction steps. To overcome such issues and demonstrate our main goal of a stable and practical chemical hydrogen storage and release with efficient H_2 storage–release cycles (Fig. 4b), we tested different lysinate salts (LysM, M = K, Na, Li; Fig. 4c and Supplementary Table 12), due to the excellent performance of LysK in capturing CO_2 (Table 2, entry 10). Indeed, LysK, LysNa and LysLi led to much higher CO_2 retention (>99.9%) during the H_2 evolution process compared with Lys (Supplementary Figs. 35–37). Hence, applying LysM instead of Lys, the H_2 evolution efficiency reached ≥80% (LysK), ≥60% (LysNa) and ≥46% (LysLi), respectively, in ten charge–discharge cycles. The observed cation-based effect is consistent with the observation of a previous work for the hydrogenation of imines, where potassium tert-butoxide led to a higher hydrogenation rate than the sodium one[47]. Notably, CO_2 reloading was not necessary in H_2 storage–release cycles applying LysM, thus greatly simplifying the process. After one cycle of hydrogen release and storage, 4.6 mmol formate (92%) was obtained applying 5 mmol LysK. As a prototype example (0.31 autoclave), the H_2 evolution process applying LysK was scaled up to 90.0 mmol without obvious drop of the efficiency in at least ten charge–discharge cycles (Fig. 4d and Supplementary Table 13), demonstrating its applicability.

Mechanistic investigations

To understand both catalyst and CO_2 capture efficiency, we tried to detect the main reaction intermediates. Thus, we performed stoichiometric reactions in Young–NMR tubes and analysed them by in situ NMR (Fig. 5a). After adding LysK (1.0 equivalent) to the solution of Mn-5 in THF-d^8:D_2O (0.4:0.1 ml) at room temperature, a new signal at 131.3 ppm in ^{31}P NMR was observed, which is assigned to I-1 (ref. [48]). Next, this mixture was pressurized with H_2 (0.5 bar), and a Mn–H species was identified with new signals of ^{31}P NMR at 162.2 ppm and ^{1}H NMR at −5.99 ppm (J_{H-P} = 51.0 Hz, triplet, J_{H-P}: H–P coupling constant), which is in accordance with a similar hydride complex previously reported[47–49]. After adding CO_2 (0.5 bar) to the tube, a weak signal at 136.9 ppm (^{31}P NMR) and 8.73 ppm (^{1}H NMR) appeared, corresponding to the Mn–OOCH species that is considered to be poorly soluble[33], meanwhile the hydride signals at 162.2 ppm (^{31}P NMR) and −5.99 ppm (^{1}H NMR) disappeared. Alternatively, by adding FA (1.0 equivalent) to the mixture of Mn-5 and LysK, a similar peak was observed (Supplementary Figs. 42–49). Control experiments of CO_2 hydrogenation in the presence of various lysine derivatives (Supplementary Table 15) revealed the presence of the α-amino acid group and an appropriate basic side chain in the amine molecule that are crucial for both the Mn-catalysed CO_2 hydrogenation reaction and CO_2 capture processes.

On the basis of the in situ NMR studies, control experiments above and the previously reported research work[33,47–49], we propose the following catalytic cycle on the reversible CO_2 hydrogenation catalysed by Mn–PN^{5}P^{iPr} complexes (Fig. 5b). The catalyst precursor is first activated by an excess of LysK via N–H deprotonation and dearomatisation of the triazine moiety, leading to active species I-1, which is described as a bimetallic Mn–K species[50,51]. During the H_2 storage step (green pathway), dihydrogen is activated via heterolytic cleavage resulting in a Mn-hydride species I-2 and transforming LysK into Lys. After insertion of C = O bond in CO_2 to Mn–H I-2, the Mn–OOCH intermediate I-3 is formed. Then, HCOOH is liberated by transforming 1 equivalent of Lys to LysK, which regenerates the active species I-1 after dearomatisation of the triazine moiety. The reverse reaction (pink pathway) enables the HCOOH dehydrogenation to H_2 and CO_2, accordingly.

Conclusions

The present work describes a concept for carbon neutral hydrogen storage and release. Utilizing a molecularly defined manganese

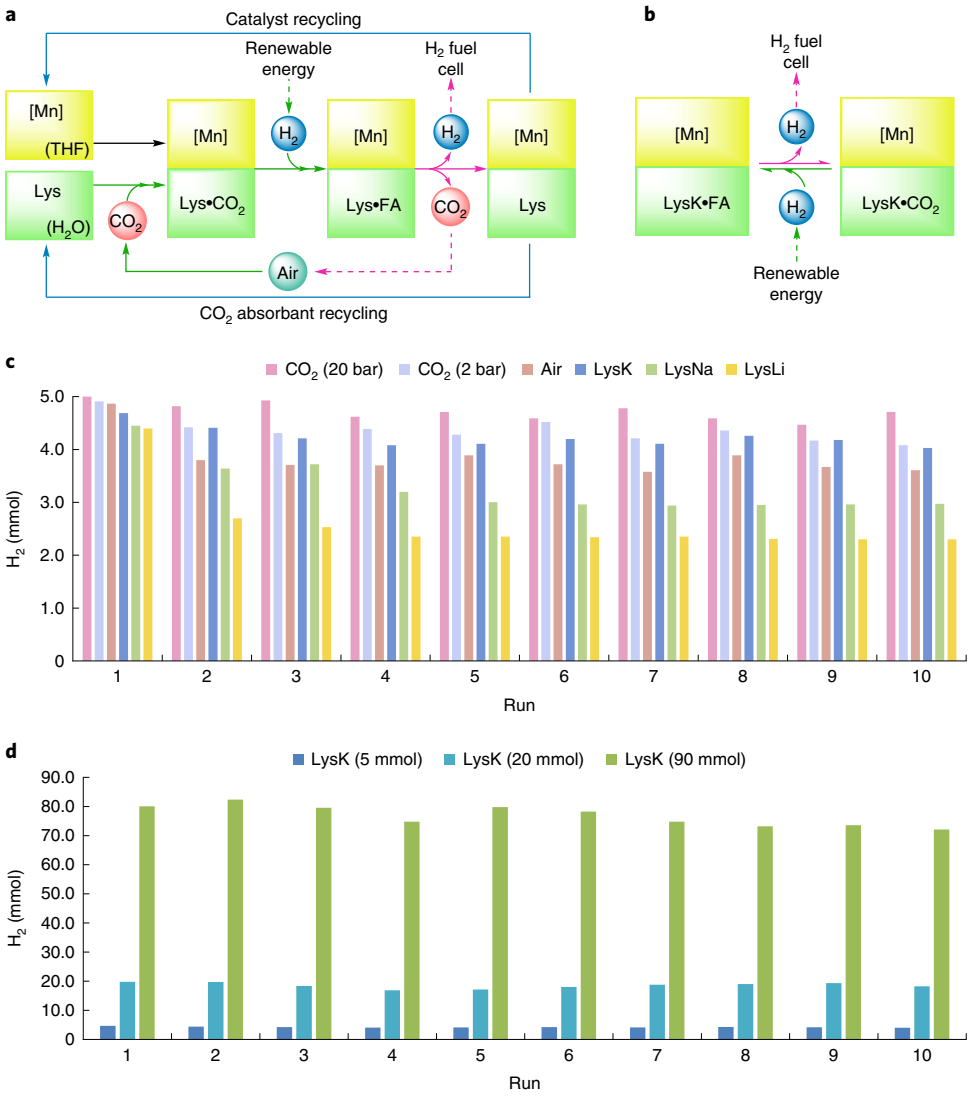

Fig. 4 | Lysine- and Mn-promoted carbon-neutral chemical hydrogen storage and release cycles. a,**b**, Illustration of the carbon-neutral hydrogen storage and release applied with Lys, including CO_2 capture from air (**a**) and the simplified hydrogen storage and release system based on LysK without CO_2 reloading (**b**). **c**,**d**, H_2 evolution in the H_2 storage–release cycles combined with CO_2 capture using Lys; CO_2 is reloaded in each cycle after H_2 release with either pure CO_2 (20 bar or 2 bar) or air. H_2 evolution using LysM (M = K, Na, Li) without CO_2 reloading (**c**). H_2 evolution in upscaled H_2 storage–release cycles applying 5.0 mmol, 20.0 mmol and 90.0 mmol LysK without CO_2 reloading (**d**).

complex in the presence of naturally occurring Lys, high efficiency for direct CO_2 hydrogenation to formate is achieved (93% yield; 2,000,000 TTON). On the other hand, the same system promotes H_2 generation from FA in the presence of Lys with >99% yield and a TTON of 600,000. This reaction system exhibited high stability and reusability. On the basis of these results, the combination of the individual processes was realised. Notably, we performed such hydrogen storage–release cycles without the addition of extra AA, catalyst and especially CO_2 due to the excellent CO_2 capture effect (99.9%) of LysK.

It is noteworthy that the CO content in the produced H_2 gas was below 10 ppm throughout the process. We successfully scaled up this method without obvious drop of the productivity in at least ten charge–discharge cycles. The current methodology represents one of the most productive combinations of CO_2 valorization and FA dehydrogenation applying homogeneous non-noble metal-based catalysts. The results inspire further research towards practical applications and pave the way for building up a carbon-neutral chemical hydrogen storage and release set-up by employing non-hazardous AAs and benign catalysts.

Methods

Materials and characterization methods. Reagents were purchased from commercial suppliers and used without further purification, including L-lysine (fluorochem, 97%), L-arginine (Alfa Aesar, >98%), L-tyrosine (Tokyo Chemical Industry (TCI), >98.5%), L-threonine (TCI, >99%), L-methionine (Alfa Aesar, >98%), L-glutamic acid (TCI, >99%), L-serine (TCI, >99%), L-proline (Acros Organics, >99%), L-cysteine (TCI, >98%), L-histidine (Sigma-Aldrich, >99%), L-tryptophan (TCI, >98.5%), glycine (Merck, >99.7%), L-glutamine (TCI, >99%), L-norleucine (TCI, >99%), 1,5-diaminopentane (TCI, >98%), 6-aminohexanoic acid (Alfa Aesar, 99%), 2,3-diaminopropanoic acid (fluorochem, 95%), N^{α}-(*t*-butoxycarbonyl)-Lys (fluorochem, 95%), N^{ε}-(*t*-butoxycarbonyl)-Lys (fluorochem, 97%), tetramethylguanidine (Alfa Aesar, 99%), L-lysine methyl ester (Alfa Aesar, 99%), pentaethylenehexamine (Sigma-Aldrich, >98%), 1,4-diazabicyclo[2.2.2]octane (TCI, > 98%), 1,8-diazabicyclo[5.4.0]undec-7-ene (DBU, TCI, > 98%), 1-butylamine (Acros Organics, 99.5%), FA (FA, Sigma-Aldrich, 98%), potassium bicarbonate (Sigma-Aldrich, 99.5%), potassium hydroxide (Fisher Chemical, 86.4%), sodium hydroxide (Fisher Chemical, 99.3%), lithium hydroxide (Sigma-Aldrich, 98%), deuterium oxide (Deutero, D-99.9%), tetrahydrofuran-d^8 (Deutero, D-99.5%), $Mn(CO)_5Br$ (Stream, 98%), H_2 (Air Liquide, grade 5.0) and CO_2 (Linde, grade 4.8). Organic solvents were collected from an SPS (Solvent Purification System) machine and stored under argon with drying reagent (molecular sieve). Deionized (DI) water was used for CO_2 capture and hydrogenation/dehydrogenation reactions. Organometallic complexes Mn-1

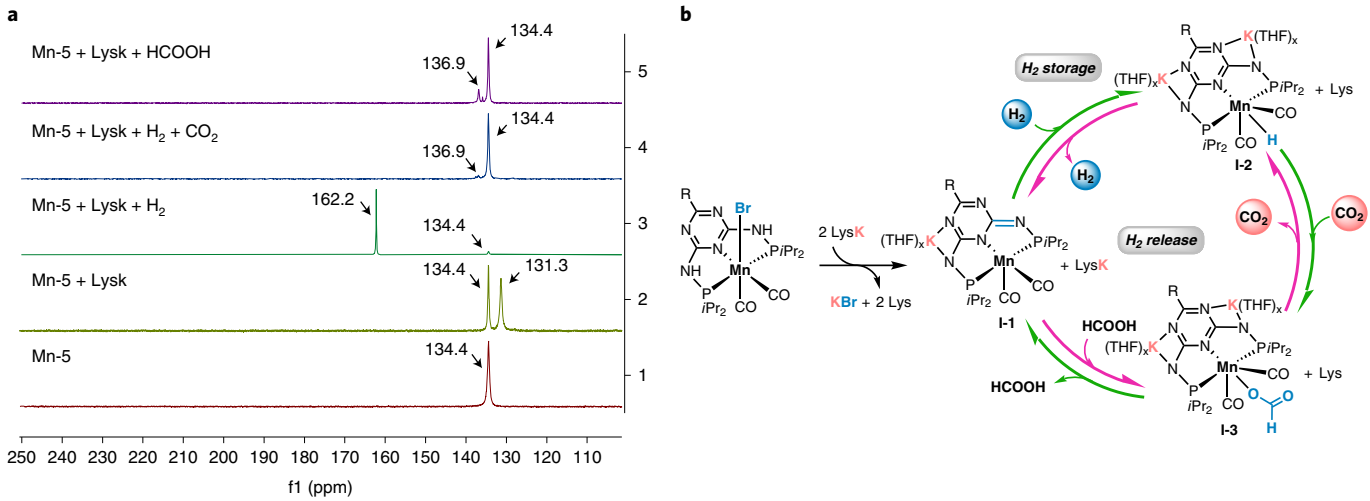

Fig. 5 | Mechanistic investigations. a,**b**, In situ ^{31}P NMR studies in Young-NMR tubes (f1: chemical shifts are shown in ppm); **a**) and the proposed catalytic cycle for reversible CO_2 hydrogenation catalysed by Mn-PN^{5}P^{iPr} complexes (**b**).

(refs. [28,52]), Mn-2 (refs. [28,52]), Mn-3 (refs. [46,53]), Mn-4 (ref. [45]), Mn-5 (ref. [29]), Mn-6 (ref. [29]), Mn-7 (ref. [29]), Mn-8 (ref. [54]), Mn-9 (refs. [45,54]), Mn-10 (ref. [55]), Mn-11 (ref. [56]), Mn-12 (ref. [34]), Fe-1 (ref. [57]), Fe-2 (ref. [57]), Fe-3 (refs. [58,59]), Co-1 (ref. [60]) and Re-1 (refs. [61,62]) were synthesized according to the corresponding publications and stored under argon with light exclusion. The manganese, rhenium and cobalt complexes were prepared by adding $Mn(CO)_5Br$ (137.4 mg, 0.5 mmol), $Re(CO)_5Br$ (203.1 mg, 0.5 mmol) or $CoBr_2$ (109.4 mg, 0.5 mmol) in THF (10 ml), respectively, dropwise to 1.1 equivalenent corresponding ligands in THF then heated and stirred at 100 °C for 20 h under argon. The reaction mixture was cooled to room temperature and concentrated in vacuo. The crude mixture was then thoroughly washed with pentane and dried under vacuum, yielding the corresponding complexes as powder (yellow for manganese complexes, white for rhenium complex and purple for cobalt complex). Fe-3 is prepared by adding 1.1 equivalent corresponding ligands in THF to anhydrous $FeBr_2$ (107.8 mg, 0.5 mmol) in THF (10 ml), and the argon inside the flask was replaced with CO by performing freeze–pump–thaw cycles. The solution was stirred at room temperature for 4 h, followed by removal of solvent under vacuum. The resulting residue was washed with pentane and dried under vacuum to generate the corresponding compound as a blue powder. Fe-2 and Fe-3 were prepared by adding 1 and 5 equivalent of $NaBH_4$ (18.9 mg, 0.5 mmol and 94.6 mg, 2.5 mmol), respectively, into Fe-3 (274.5 mg, 0.5 mmol) in EtOH (35 ml). The reaction mixture was then stirred for 5 h at room temperature. The solvent was removed in vacuo and the residue dissolved in toluene. The resulting suspension was filtered through a short pad of celite. The filtrate was concentrated in vacuo and the resulting solid washed thoroughly with pentane to create a yellow powder. Unless otherwise stated, all reactions were conducted under an argon atmosphere. ^{1}H, ^{13}C and ^{31}P NMR spectroscopy were recorded using Bruker AV 300 MHz and Bruker AV 400 MHz spectrometers. All NMR data are expressed as chemical shift in ppm. ^{1}H and ^{13}C NMR chemical shifts were determined relative to the internal standard DMF (7.92 ppm and 165.53 ppm, respectively) or 1,4-dioxane (3.75 ppm and 67.19 ppm, respectively) in D_2O. ^{31}P NMR spectra were calibrated with an external H_3PO_4 standard (0 ppm). ^{13}C NMR-quant measurements were performed with a Bruker AV 400 MHz spectrometer, relaxation delay = 20 s (relaxation delay > 20 s did not change the integration), number of scans = 512, acquisition time = 1.1141 s (refs. [63–66]). NMR spectra were interpreted and processed using MestReNova (version 14.0.1–23559). Gas chromatography (Agilent Technologies 7890 A GC system, Carboxen/TCD) was used to analyse the content of the gas phase with a CO quantification limit of 10 ppm. pH values were measured on a laboratory digital pH meter (Mettler–Toledo AG, SevenEasy pH 8603) at room temperature (24 °C).

Measurement of formate yield in the hydrogenation of CO_2. The respective amount of catalyst (0.10 µmol or 0.02 µmol) was dispensed from the stock solution; Lys (5.0 mmol), THF (5 ml) and H_2O (5 ml) were added to a 50 ml autoclave equipped with a magnetic stir bar. After pressurizing the reactor with CO_2 and H_2 gas, the reaction mixture was heated and stirred on a pre-heated oil bath for 12 h. Then the reactor was cooled to room temperature and the inside pressure was carefully released. A biphasic reaction mixture was obtained containing a transparent organic upper layer and an aqueous yellow lower layer. Addition of DI water (~3 ml) to the above-mentioned mixture resulted in a homogeneous solution (Supplementary Figs. 3–4) (ref. [42]). DMF (250 µl, 3.24 mmol) was added as an internal standard to the reaction mixture. The reaction mixture was then analysed by ^{1}H NMR with a few drops of D_2O (~1 ml) to lock the signals[34]. Yield of formate is calculated by (mmol formate)/(mmol Lys) × 100%. TON of formate is calculated by (mmol formate)/(mmol catalyst). The gas mixtures were analysed by GC, and no concomitant of CO/CH_4 was found.

Measurement of H_2 yield in the FA dehydrogenation. Appropriate amount of catalyst (0.10–0.20 µmol) was dispensed from the stock solution, FA (5.0 mmol), Lys (5.0 mmol), THF (5 ml) and H_2O (5 ml) were added to a 100 ml autoclave equipped with a magnetic stir bar. The reaction mixture was then heated and stirred on a pre-heated oil bath for 12 h. The reactor was cooled to room temperature, and the inside pressure was released carefully to the manual burettes. A 5 ml degassed syringe was used to obtain a gas sample analysed by GC. CO is not detectable in all cases (below the CO quantification limit of 10 ppm). Yield of H_2 is calculated by (mmol H_2)/(mmol HCOOH) × 100%. TON of H_2 is calculated by (mmol H_2)/(mmol catalyst).

Calculation of the hydrogen volume, mole, yield and TON. The gas evolution was corrected with the blank volume (18 ml), which corresponds to the gas evolution of the reaction without any catalyst. H_2 volume, V_{H_2}, and CO_2 volume, V_{CO_2}, are calculated with the following equation:

$$V_{H_2} = (V_{obs} - V_{blank}) \times \frac{\%V_{H_2}}{\%V_{H_2} + \%V_{CO_2}} \quad (1)$$

$$V_{CO_2} = (V_{obs} - V_{blank}) \times \frac{\%V_{CO_2}}{\%V_{H_2} + \%V_{CO_2}} \quad (2)$$

Moles of H_2, n_{H_2}, and moles of CO_2, n_{CO_2}, are calculated with the following equation:

$$n_{H_2} = \frac{V_{H_2}}{V_{m_{H_2}(25\,^\circ C)}} \quad (3)$$

$$n_{CO_2} = \frac{V_{CO_2}}{V_{m_{CO_2}(25\,^\circ C)}} \quad (4)$$

Hydrogen yield Y_{H_2} is calculated with the following equation:

$$Y_{H_2} = \frac{n_{H_2}}{n_{FA}} \times 100\% \quad (5)$$

The turnover number (TON) of H_2 is calculated with the following equation:

$$TON = \frac{n_{H_2}}{n_{cat}} \quad (6)$$

V_{obs} is the gas evolution volume of the catalytic reaction measured in the manual burettes. V_{blank} is the gas evolution volume of the blank reaction measured in the manual burettes. $\%V_{H_2}$ and $\%V_{CO_2}$ are the volume ratios of H_2 and CO_2, respectively, determined by GC. n_{FA} and n_{cat} are the moles of FA and catalyst, respectively. $V_{m_{H_2}(25\,^\circ C)}$ and $V_{m_{CO_2}(25\,^\circ C)}$ are the molar volumes of H_2 and CO_2

at room temperature (25 °C), respectively, calculated with the Van Der Waals equation (below).

Calculation of H_2 molar volume $V_{m_{H_2(25^\circ C)}}$:

$$V_{m_{H_2(25^\circ C)}} = \frac{R \times T}{p} + b - \frac{a}{R \times T} = 24.48 \quad (7)$$

Where $R = 8.3145\ m^3 \cdot Pa \cdot mol^{-1} \cdot K^{-1}$, $T = 273.15 +$ room temperature (°C) K, $P = 101325$ Pa, $a = 24.9 \times 10^{-3}\ Pa \cdot m^6 \cdot mol^{-2}$, $b = 26.7 \times 10^{-6}\ m^3 \cdot mol^{-1}$.

Calculation of CO_2 molar volume $V_{m_{CO_2(25^\circ C)}}$:

$$V_{m_{CO_2(25^\circ C)}} = \frac{R \times T}{p} + b - \frac{a}{R \times T} = 24.36 \quad (8)$$

where $R = 8.3145\ m^3\ Pa\ mol^{-1}\ K^{-1}$, $T = 273.15 +$ room temperature (°C) (K), $P = 101{,}325$ Pa, $a = 36.5 \times 10^{-2}\ Pa\ m^6\ mol^{-2}$ and $b = 42.7 \times 10^{-6}\ m^3\ mol^{-1}$.

Catalyst recycling studies in CO_2 hydrogenation. Catalyst Mn-6 (0.02 µmol, dispensed from the stock solution), Lys (730.9 mg, 5.0 mmol), THF (5 ml) and H_2O (5 ml) were added to a 50 ml autoclave equipped with a magnetic stir bar. After pressurizing the reactor with CO_2 (20 bar) and H_2 (60 bar) gas, the reaction mixture was heated and stirred on a pre-heated oil bath at 115 °C for 12 h. Then the reactor was cooled to room temperature, and the inside pressure was carefully released. A biphasic reaction mixture was obtained containing a transparent organic upper layer and an aqueous yellow lower layer (Supplementary Fig. 26). After the separation of the two layers, the aqueous lower layer was washed and extracted with additional THF (1 ml × 2), and the combined organic parts were used directly for the next run by adding a new batch of 5.0 mmol Lys. Meanwhile, DMF (250 µl, 3.24 mmol) was added into the aqueous lower layer as an internal standard, then analysed by ^1H NMR with a few drops of D_2O (~1 ml) to lock the signals[34]. A total of ten runs of CO_2 hydrogenation to formate were performed by using the above-mentioned procedure. Yield of formate is calculated by (mmol formate)/(mmol Lys) × 100%. TON of formate is calculated by (mmol formate)/(mmol catalyst). The gas mixtures were analysed by GC, and no concomitant of CO/CH_4 was found.

Catalyst recycling studies in FA dehydrogenation. Catalyst Mn-6 (0.1 mg, 0.17 µmol), FA, Lys (730.9 mg, 5.0 mmol), THF (5 ml) and H_2O (5 ml) were added to a 100 ml autoclave equipped with a magnetic stir bar. The reaction mixture was then heated and stirred on a pre-heated oil bath for 12 h. The reactor was cooled to room temperature and the inside pressure was released carefully to the manual burettes, and the content of the gas phase was analysed by GC. CO was not detectable in all cases (below the CO quantification limit of 10 ppm). After each run, a new batch of FA (first to fifth runs: 5.0 mmol FA and sixth to tenth runs: 20.0 mmol FA) was loaded into the reaction mixture, then heated and stirred on a pre-heated oil bath for 12 h. Following this procedure, a total of ten runs of catalytic dehydrogenation of FA in the presence of Lys were performed. Yield of H_2 is calculated by (mmol H_2)/(mmol HCOOH) × 100%. TON of H_2 is calculated by (mmol H_2)/(mmol catalyst).

Measurement of hydrogen evolution in the H_2 storage–release cycles applying Lys combined with CO_2 capture. The H_2 storage–release cycles start from the dehydrogenation of FA (H_2 release): Mn-6 (0.1 mg, 0.17 µmol), FA (188.6 µl, 5.0 mmol), Lys (730.9 mg, 5.0 mmol), THF (5 ml) and H_2O (5 ml) were added to a 100 ml autoclave equipped with a magnetic stir bar. The reaction mixture was then heated and stirred on a pre-heated oil bath at 90 °C for 12 h. The reactor was cooled to room temperature, and the inside pressure was released carefully to the manual burettes. The content of the gas phase was analysed by GC. CO was not detectable in all cases (below the CO quantification limit of 10 ppm). Then CO_2 is replenished under the following conditions—capture with CO_2 (20 bar or 2 bar): after the completion of the above-mentioned FA dehydrogenation, the 100 ml autoclave was charged with CO_2 (20 bar for 0.5 h or 2 bar for 6 h). After releasing the overpressure of CO_2, the 100 ml autoclave was filled with 80 bar of H_2. Then the reaction mixture was heated and stirred on a pre-heated oil bath at 85 °C for 12 h. Afterwards, the reactor was cooled to room temperature, and the inside pressure was released carefully. Then the autoclave was subjected to the H_2 release procedure. Following this procedure, a total of ten runs were performed via CO_2 recharging under 20 bar or 2 bar of CO_2. Capture from ambient air: after the completion of FA dehydrogenation, a biphasic reaction mixture containing a transparent organic upper layer and a pale yellow aqueous lower layer was obtained. After the separation of the two layers, the aqueous lower layer was washed with additional THF (1 ml × 2), and the combined organic layer was reserved for the following H_2 storage step. On the other hand, the aqueous layer was subjected to CO_2 capture from ambient air at room temperature for 24 h. After bubbling with argon for 0.5 h, this aqueous layer was combined with the above-mentioned organic layer and loaded to a 100 ml autoclave. The autoclave was then filled with 80 bar of H_2 and heated and stirred on a pre-heated oil bath at 85 °C for 12 h. The reactor was cooled to room temperature, and the inside pressure was released carefully. Then the autoclave was subjected to the H_2 release procedure. Following this procedure, a total of ten runs were performed with CO_2 capture from ambient air. It should be noted that no H_2 evolution was observed at room temperature in the H_2 storage–release cycles for up to 12 h.

Measurement of hydrogen evolution in the H_2 storage–release cycles applying LysM (without CO_2 reloading). The lysinate salts (LysM, 5.0 mmol) was prepared via stirring Lys (5.0 mmol) with 1.0 equivalent of corresponding alkali metal hydroxides MOH (KOH, NaOH, LiOH) for 30 min in 1 ml DI water at room temperature before the H_2 storage–release cycles. The H_2 storage–release cycles start from the dehydrogenation of FA (H_2 release): Mn-6 (0.1 mg, 0.17 µmol), FA (188.6 µl, 5.0 mmol), LysM (5.0 mmol), THF (5 ml) and H_2O (4 ml) were added to a 100 ml autoclave equipped with a magnetic stir bar. The reaction mixture was then heated and stirred on a pre-heated oil bath at 90 °C for 12 h. The reactor was cooled to room temperature, and the inside pressure was released carefully to the manual burettes and the content of the gas phase was analysed by GC. CO was not detectable in all cases (below the CO quantification limit of 10 ppm). After the completion of FA dehydrogenation, the 100 ml autoclave was filled with 80 bar of H_2. Then the reaction mixture was heated and stirred on a pre-heated oil bath at 85 °C for 12 h. Afterwards, the reactor was cooled to room temperature, and the inside pressure was released carefully to the manual burettes and the content of the gas phase was analysed by GC. CO was not detectable in all cases (below the CO quantification limit of 10 ppm). After the completion of FA dehydrogenation, the 100 ml autoclave was filled with 80 bar of H_2. Then the reaction mixture was heated and stirred on a pre-heated oil bath at 85 °C for 12 h. Afterwards, the reactor was cooled to room temperature, and the inside pressure was released carefully. Then the autoclave was subjected to the H_2 release procedure. Following this procedure, a total of ten runs were performed with 5.0 mmol LysK, LysNa, and LysLi.

Measurement of hydrogen evolution in the up-scaled H_2 storage–release cycles applying LysK (without CO_2 reloading). The 20.0 mmol lysine potassium salt (LysK, 20.0 mmol) was prepared via stirring Lys (2,923.8 mg, 20.0 mmol) with 1.0 equivalent of KOH for 30 min in 10 ml DI water at room temperature before the H_2 storage–release cycles. The H_2 storage-release cycles start from the dehydrogenation of FA (H_2 release); Mn-6 (0.4 mg, 0.68 µmol), FA:LysK (20.0:20.0 mmol), THF (20 ml) and H_2O (10 ml) were added to a 300 ml autoclave equipped with a magnetic stir bar. The reaction mixture was then heated and stirred on a pre-heated oil bath at 90 °C for 12 h. The reactor was cooled to room temperature, and the inside pressure was released carefully to the manual burettes and the content of the gas phase was analysed by GC. CO is not detectable in all cases (below the CO quantification limit of 10 ppm). After the completion of FA dehydrogenation, the 300 ml autoclave was filled with 80 bar of H_2. Then the reaction mixture was heated and stirred on a pre-heated oil bath at 85 °C for 12 h. Afterwards, the reactor was cooled to room temperature, and the inside pressure was released carefully. Then the autoclave was subjected to the H_2 release procedure. Following this procedure, a total of ten runs were performed with LysK in 20.0 mmol scale. The 90 mmol lysine potassium salt (LysK, 90.0 mmol) was prepared via stirring Lys (90.0 mmol) with 1.0 equivalent of KOH for 30 min in 20 ml DI water at room temperature before the H_2 storage–release cycles. The H_2 storage–release cycles started from the dehydrogenation of FA (H_2 release); Mn-6 (1.8 mg, 3.05 µmol), FA:LysK (90.0:90.0 mmol), THF (30 ml) and H_2O (60 ml) were added to a 300 ml autoclave equipped with a magnetic stir bar. The reaction mixture was then heated and stirred on a pre-heated oil bath at 90 °C for 12 h. The reactor was cooled to room temperature, and the inside pressure was released carefully to the manual burettes and the content of the gas phase was analysed by GC. CO was not detectable in all cases (below the CO quantification limit of 10 ppm). After the completion of FA dehydrogenation, the 300 ml autoclave was filled with 80 bar of H_2. Then the reaction mixture was heated and stirred on a pre-heated oil bath at 85 °C for 12 h. Afterwards, the reactor was cooled to room temperature, and the inside pressure was released carefully. Then the autoclave was subjected to the H_2 release procedure. Following this procedure, a total of ten runs were performed with LysK at 90.0 mmol scale.

Data availability

All the relevant data are included in the published article and its Supplementary Information.

Received: 2 December 2021; Accepted: 30 March 2022;
Published online: 19 May 2022

References

1. Tans, P. Trends in atmospheric carbon dioxide. NOAA/GML https://gml.noaa.gov/ccgg/trends/ (2022).
2. Keeling, R. Carbon dioxide measurements. Scripps Institution of Oceanography https://scrippsco2.ucsd.edu/ (2022).
3. Roger, I., Shipman, M. A. & Symes, M. D. Earth-abundant catalysts for electrochemical and photoelectrochemical water splitting. *Nat. Rev. Chem.* **1**, 0003 (2017).
4. Schneidewind, J., Argüello Cordero, M. A., Junge, H., Lochbrunner, S. & Beller, M. Two-photon, visible light water splitting at a molecular ruthenium complex. *Energy Environ. Sci.* **14**, 4427–4436 (2021).
5. Yadav, M. & Xu, Q. Liquid-phase chemical hydrogen storage materials. *Energy Environ. Sci.* **5**, 9698–9725 (2012).

6. Chatterjee, S., Dutta, I., Lum, Y., Lai, Z. & Huang, K.-W. Enabling storage and utilization of low-carbon electricity: power to formic acid. *Energy Environ. Sci.* **14**, 1194–1246 (2021).
7. Mellmann, D., Sponholz, P., Junge, H. & Beller, M. Formic acid as a hydrogen storage material—development of homogeneous catalysts for selective hydrogen release. *Chem. Soc. Rev.* **45**, 3954–3988 (2016).
8. Onishi, N., Laurenczy, G., Beller, M. & Himeda, Y. Recent progress for reversible homogeneous catalytic hydrogen storage in formic acid and in methanol. *Coord. Chem. Rev.* **373**, 317–332 (2018).
9. Sordakis, K. et al. Homogeneous catalysis for sustainable hydrogen storage in formic acid and alcohols. *Chem. Rev.* **118**, 372–433 (2018).
10. Leitner, W., Dinjus, E. & Gaßner, F. Activation of carbon dioxide: IV. Rhodium-catalysed hydrogenation of carbon dioxide to formic acid. *J. Organomet. Chem.* **475**, 257–266 (1994).
11. Boddien, A. et al. CO_2-"neutral" hydrogen storage based on bicarbonates and formates. *Angew. Chem.* **50**, 6411–6414 (2011).
12. Papp, G., Csorba, J., Laurenczy, G. & Joó, F. A charge/discharge device for chemical hydrogen storage and generation. *Angew. Chem.* **50**, 10433–10435 (2011).
13. Boddien, A. et al. Towards the development of a hydrogen battery. *Energy Environ. Sci.* **5**, 8907–8911 (2012).
14. Filonenko, G. A., van Putten, R., Schulpen, E. N., Hensen, E. J. M. & Pidko, E. A. Highly efficient reversible hydrogenation of carbon dioxide to formates using a ruthenium PNP-pincer catalyst. *ChemCatChem* **6**, 1526–1530 (2014).
15. Hsu, S.-F. et al. A rechargeable hydrogen battery based on Ru catalysis. *Angew. Chem.* **53**, 7074–7078 (2014).
16. Kothandaraman, J. et al. Amine-free reversible hydrogen storage in formate salts catalyzed by ruthenium pincer complex without pH control or solvent change. *ChemSusChem* **8**, 1442–1451 (2015).
17. Sordakis, K., Dalebrook, A. F. & Laurenczy, G. A viable hydrogen storage and release system based on cesium formate and bicarbonate salts: mechanistic insights into the hydrogen release step. *ChemCatChem* **7**, 2332–2339 (2015).
18. Xin, Z. et al. Towards hydrogen storage through an efficient ruthenium-catalyzed dehydrogenation of formic acid. *ChemSusChem* **11**, 2077–2082 (2018).
19. Hull, J. F. et al. Reversible hydrogen storage using CO_2 and a proton-switchable iridium catalyst in aqueous media under mild temperatures and pressures. *Nat. Chem.* **4**, 383–388 (2012).
20. Tanaka, R., Yamashita, M., Chung, L. W., Morokuma, K. & Nozaki, K. Mechanistic studies on the reversible hydrogenation of carbon dioxide catalyzed by an Ir-PNP complex. *Organometallics* **30**, 6742–6750 (2011).
21. Forberg, D. et al. Single-catalyst high-weight% hydrogen storage in an *N*-heterocycle synthesized from lignin hydrogenolysis products and ammonia. *Nat. Commun.* **7**, 13201 (2016).
22. Enthaler, S. et al. Exploring the reactivity of nickel pincer complexes in the decomposition of formic acid to CO_2/H_2 and the hydrogenation of $NaHCO_3$ to HCOONa. *ChemCatChem* **7**, 65–69 (2015).
23. Jessop, P. G., Joó, F. & Tai, C.-C. Recent advances in the homogeneous hydrogenation of carbon dioxide. *Coord. Chem. Rev.* **248**, 2425–2442 (2004).
24. Bernskoetter, W. H. & Hazari, N. Reversible hydrogenation of carbon dioxide to formic acid and, ethanol: Lewis acid enhancement of base metal catalysts. *Acc. Chem. Res.* **50**, 1049–1058 (2017).
25. Alig, L., Fritz, M. & Schneider, S. First-row transition metal (de) hydrogenation catalysis based on functional pincer ligands. *Chem. Rev.* **119**, 2681–2751 (2019).
26. Wei, D. & Darcel, C. Iron catalysis in reduction and hydrometalation reactions. *Chem. Rev.* **119**, 2550–2610 (2019).
27. Valyaev, D. A., Lavigne, G. & Lugan, N. Manganese organometallic compounds in homogeneous catalysis: past, present, and prospects. *Coord. Chem. Rev.* **308**, 191–235 (2016).
28. Elangovan, S. et al. Selective catalytic hydrogenations of nitriles, ketones and aldehydes by well-defined manganese pincer complexes. *J. Am. Chem. Soc.* **138**, 8809–8814 (2016).
29. Kallmeier, F., Irrgang, T., Dietel, T. & Kempe, R. Highly active and selective manganese C=O bond hydrogenation catalysts: the importance of the multidentate ligand, the ancillary ligands, and the oxidation state. *Angew. Chem.* **55**, 11806–11809 (2016).
30. Mukherjee, A. & Milstein, D. Homogeneous catalysis by cobalt and manganese pincer complexes. *ACS Catal.* **8**, 11435–11469 (2018).
31. Wang, Y., Wang, M., Li, Y. & Liu, Q. Homogeneous manganese-catalyzed hydrogenation and dehydrogenation reactions. *Chem* **7**, 1180–1223 (2021).
32. Azouzi, K., Valyaev, D. A., Bastin, S. & Sortais, J.-B. Manganese—new prominent actor in transfer hydrogenation catalysis. *Curr. Opin. Green Sustain. Chem.* **31**, 100511 (2021).
33. Bertini, F. et al. Carbon dioxide hydrogenation catalysed by well-defined Mn (I) PNP pincer hydride complexes. *Chem. Sci.* **8**, 5024–5029 (2017).
34. Dubey, A., Nencini, L., Fayzullin, R. R., Nervi, C. & Khusnutdinova, J. R. Bio-inspired Mn(I) complexes for the hydrogenation of CO_2 to formate and formamide. *ACS Catal.* **7**, 3864–3868 (2017).
35. Kumar, A. et al. CO_2 activation by manganese pincer complexes through different modes of metal–ligand cooperation. *Dalton Trans.* **48**, 14580–14584 (2019).
36. Kostera, S. et al. Carbon dioxide hydrogenation to formate catalyzed by a bench-stable, non-pincer-type Mn(I) alkylcarbonyl complex. *Organometallics* **40**, 1213–1220 (2021).
37. Schlenker, K. et al. Role of ligand-bound CO_2 in the hydrogenation of CO_2 to formate with a (PNP)Mn catalyst. *ACS Catal.* **11**, 8358–8369 (2021).
38. Tondreau, A. M. & Boncella, J. M. 1,2-Addition of formic or oxalic acid to $^{-}N\{CH_2CH_2(PiPr_2)\}_2$-supported Mn(I) dicarbonyl complexes and the manganese-mediated decomposition of formic acid. *Organometallics* **35**, 2049–2052 (2016).
39. Andérez-Fernández, M. et al. A stable manganese pincer catalyst for the selective dehydrogenation of methanol. *Angew. Chem.* **56**, 559–562 (2017).
40. Anderson, N. H., Boncella, J. & Tondreau, A. M. Manganese-mediated formic acid dehydrogenation. *Chem. Eur. J.* **25**, 10557–10560 (2019).
41. Léval, A. et al. Hydrogen production from formic acid catalyzed by a phosphine free manganese complex: investigation and mechanistic insights. *Green Chem.* **22**, 913–920 (2020).
42. Wei, D., Junge, H. & Beller, M. An amino acid based system for CO_2 capture and catalytic utilization to produce formates. *Chem. Sci.* **12**, 6020–6024 (2021).
43. Ghayur, A., Verheyen, T. V. & Meuleman, E. Biological and chemical treatment technologies for waste amines from CO_2 capture plants. *J. Environ. Manag.* **241**, 514–524 (2019).
44. Pandey, A. K., Pandey, K. & Singh, L. K. in *Innovations in Food Technology* (eds Mishra, P. et al.) 211–229 (Springer, 2020).
45. Papa, V. et al. Efficient and selective hydrogenation of amides to alcohols and amines using a well-defined manganese–PNN pincer complex. *Chem. Sci.* **8**, 3576–3585 (2017).
46. Borghs, J. C., Lebedev, Y., Rueping, M. & El-Sepelgy, O. Sustainable manganese-catalyzed solvent-free synthesis of pyrroles from 1,4-diols and primary amines. *Org. Lett.* **21**, 70–74 (2019).
47. Fertig, R., Irrgang, T., Freitag, F., Zander, J. & Kempe, R. Manganese-catalyzed and base-switchable synthesis of amines or imines via borrowing hydrogen or dehydrogenative condensation. *ACS Catal.* **8**, 8525–8530 (2018).
48. Freitag, F., Irrgang, T. & Kempe, R. Mechanistic studies of hydride transfer to imines from a highly active and chemoselective manganate catalyst. *J. Am. Chem. Soc.* **141**, 11677–11685 (2019).
49. Kallmeier, F., Dudziec, B., Irrgang, T. & Kempe, R. Manganese-catalyzed sustainable synthesis of pyrroles from alcohols and amino alcohols. *Angew. Chem.* **56**, 7261–7265 (2017).
50. Zhang, G., Irrgang, T., Schlagbauer, M. & Kempe, R. Synthesis of 1,3-diketones from esters via liberation of hydrogen. *Chem. Catal.* **1**, 681–690 (2021).
51. Schlagbauer, M., Kallmeier, F., Irrgang, T. & Kempe, R. Manganese-catalyzed β-methylation of alcohols by methanol. *Angew. Chem.* **59**, 1485–1490 (2020).
52. Elangovan, S. et al. Efficient and selective *N*-alkylation of amines with alcohols catalysed by manganese pincer complexes. *Nat. Commun.* **7**, 12641 (2016).
53. Xia, T. et al. Manganese PNP-pincer catalyzed isomerization of allylic/homo-allylic alcohols to ketones—activity, selectivity, efficiency. *Catal. Sci. Technol.* **9**, 6327–6334 (2019).
54. Kaithal, A., Hölscher, M. & Leitner, W. Catalytic hydrogenation of cyclic carbonates using manganese complexes. *Angew. Chem.* **57**, 13449–13453 (2018).
55. Perez, M., Elangovan, S., Spannenberg, A., Junge, K. & Beller, M. Molecularly defined manganese pincer complexes for selective transfer hydrogenation of ketones. *ChemSusChem* **10**, 83–86 (2017).
56. van Putten, R. et al. Non-pincer-type manganese complexes as efficient catalysts for the hydrogenation of esters. *Angew. Chem.* **56**, 7531–7534 (2017).
57. Chakraborty, S. et al. Iron-based catalysts for the hydrogenation of esters to alcohols. *J. Am. Chem. Soc.* **136**, 7869–7872 (2014).
58. Alberico, E. et al. Selective hydrogen production from methanol with a defined iron pincer catalyst under mild conditions. *Angew. Chem.* **52**, 14162–14166 (2013).
59. Werkmeister, S. et al. Hydrogenation of esters to alcohols with a well-defined iron complex. *Angew. Chem.* **53**, 8722–8726 (2014).
60. Zhou, W. et al. Cobalt-catalyzed aqueous dehydrogenation of formic acid. *Chem. Eur. J.* **25**, 8459–8464 (2019).
61. Wei, D., Roisnel, T., Darcel, C., Clot, E. & Sortais, J.-B. Hydrogenation of carbonyl derivatives with a well-defined rhenium precatalyst. *ChemCatChem* **9**, 80–83 (2017).
62. Piehl, P., Peña-López, M., Frey, A., Neumann, H. & Beller, M. Hydrogen autotransfer and related dehydrogenative coupling reactions using a rhenium(I) pincer catalyst. *Chem. Commun.* **53**, 3265–3268 (2017).
63. Barzagli, F., Mani, F. & Peruzzini, M. A ^{13}C NMR study of the carbon dioxide absorption and desorption equilibria by aqueous 2-aminoethanol and *N*-methyl-substituted 2-aminoethanol. *Energy Environ. Sci.* **2**, 322–330 (2009).

64. Barbarossa, V. et al. Efficient CO_2 capture by non-aqueous 2-amino-2-methyl-1-propanol (AMP) and low temperature solvent regeneration. *RSC Adv.* **3**, 12349–12355 (2013).
65. Perinu, C., Arstad, B. & Jens, K.-J. ^{13}C NMR experiments and methods used to investigate amine-CO_2-H_2O systems. *Energy Proc.* **37**, 7310–7317 (2013).
66. Kothandaraman, J., Goeppert, A., Czaun, M., Olah, G. A. & Prakash, G. K. S. Conversion of CO_2 from air into methanol using a polyamine and a homogeneous ruthenium catalyst. *J. Am. Chem. Soc.* **138**, 778–781 (2016).

Acknowledgements

D.W., R.S., P.S., H.J. and M.B. acknowledge financial support from the State of Mecklenburg-Vorpommern and European Union (EFRE; project 'h2cycle'). D.W., H.J. and M.B. acknowledge the Danish government for funding the CADIAC excellence cluster and the Leibniz-Program Cooperative Excellence K308/2020 (project 'SUPREME'). D.W. thanks X. Liu for providing some starting materials. We thank the analytical team of LIKAT for their kind support.

Author contributions

Investigation (performing the experiments, data collection), formal analysis and writing (original draft), D.W. and R.S.; conceptualization, funding acquisition, methodology, supervision, writing (review and editing), P.S., H.J. and M.B. All authors have read and agreed to the published version of this work. D.W. and R.S. contributed equally to the work.

Competing interests

The methods disclosed in this work have been filed as Patent application PCT/EP2022/052967 with APEX Energy Teterow GmbH as the applicant and D.W., R.S., H.J., M.B. and P.S. (employed by APEX Energy Teterow GmbH) as inventors. The status of the patent application is pending.

Additional information

Supplementary information The online version contains supplementary material available at https://doi.org/10.1038/s41560-022-01019-4.

Correspondence and requests for materials should be addressed to Peter Sponholz, Henrik Junge or Matthias Beller.

Peer review information *Nature Energy* thanks Sheri Lense, Rhett Kempe and Wan-Hui Wang for their contribution to the peer review of this work.

Reprints and permissions information is available at www.nature.com/reprints.

Publisher's note Springer Nature remains neutral with regard to jurisdictional claims in published maps and institutional affiliations.